RSC Advances

RSC Publishing

PAPER

View Article Online
View Journal | View Issue

Cite this: *RSC Advances*, 2013, **3**, 18055

The regioselectivity and synthetic mechanism of 1,2-benzimidazole squaraines: combined experimental and theoretical studies†

Guomin Xia, Zhiwei Wu, Yanli Yuan and Hongming Wang*

Received 29th May 2013,
Accepted 19th July 2013

DOI: 10.1039/c3ra43608j

www.rsc.org/advances

In this paper, a synthetic method to produce 1,2-benzimidazole squaraines with a yield of up to 89% is developed. It is found that both strong organic and inorganic bases have a satisfactory catalytic activity for this reaction. Theoretical studies provide detailed explanations for the 1,2 *versus* 1,3 condensation regiochemistry of the squaraines. The experimental and theoretical studies agree well with each other, paving a practical way to efficiently synthesize 1,2-squaraines.

Introduction

Squaraine (SQ) dyes are the product of condensation of squaric acid and two equivalents of a suitable electron-rich precursor[1] and are notable for their exceptionally high absorption coefficients extending from the green to the near-infrared region.[2,3] This has prompted their exploitation in a number of technologically relevant applications, including photoconductivity,[4] data storage,[5] light-emitting field-effect transistors,[6] solar cells[7] and fluorescent histological probes.[8] Since the pioneering work of Cohen in 1959,[9] SQs have also been used in the fields of bioorganic and medicinal chemistry as well.[10] For example, Xie *et al.* demonstrated that SQ is an effective pharmacophore for the design of tyrosine phosphatase inhibitors.[11]

The synthesis of squaraine dyes was first reported in the 1960s.[12] Since then, numerous reports describing the synthesis and properties of SQs have appeared in the recent decades.[13] According to previous investigations, SQs are the condensation product of two electron-rich derivatives (activated arenes, 2,4-dimethylpyrrole and benzothiazole) and squaric acid or their esters, which generally affords the 1,3-regioisomer as the main product and the 1,2-isomer as the by-product. Modifying the reaction conditions only slightly increases the regioselectivity toward 1,2-SQ; the reaction is regioselective and the major products are still the 1,3-isomers. Although some studies indicate that 1,2-SQ can be synthesized through a two-step Friedel–Crafts acylation reaction between squaric acid chloride and bromo-substituted thiophene, its direct synthesis from squaric acid or squarate have seldom been reported. As we all know, 1,2-SQs are considered to be promising as sensitizers in organic photoconducting devices and electron-acceptor components for the construction of high-performance D–A-type conjugated photovoltaic polymers,[14] so a facile and high selectivity route to synthesize 1,2-SQs is urgently required.

Ramaiah's group achieved the selective synthesis of 1,2- and 1,3-semisquaraine[15] and identified the 1,3-isomer as the reactive intermediate in the squaraine dye formation rather than the neutral 1,2-isomer. Their investigations indicate that the base influences the regioselectivity of 1,2- and 1,3-semisquaraine. Ronchi *et al.* identified the main electronic factors in this reaction and changed its conditions, increasing the yield of 1,2-SQs up to 66%.[16]

It is clear that the synthesis of 1,2-SQs is a significant challenge, and the yield as well as selectivity still remains unsatisfactory. In this paper, we report a synthetic method to produce 1,2-benzimidazole squaraines (**3a** and **3b**) in a high yield. To explore the reason for the high regioselectivity of **3a** and **3b**, the overall reaction mechanisms were studied by density functional theory (DFT) calculations as well. By combining the experimental and computational findings, we are able to propose a method of chemical regulation that changes the regioselectivity of the product. This work sheds light on the factors influencing the reaction *via* the 1,2- *versus* the 1,3-condensation pathway, which could provide guidelines for the synthesis of desired 1,2-SQs in the future.

Results and discussion

After considering most of the syntheses of 1,3-SQs in previous reports, we planned to produce 1,3-SQ (**2a**) by reacting a

Institute for Advanced Study, Department of Chemistry, Nanchang University, Nanchang, 330031, China. E-mail: Hongmingwang@ncu.edu.cn; Fax: 0086-791-3969552; Tel: 0086-791-3969552

† Electronic supplementary information (ESI) available: cartesian coordinates and calculated energies for all structures used in the quantum chemical calculations. CCDC number 924565. For ESI and crystallographic data in CIF or other electronic format see DOI: 10.1039/c3ra43608j

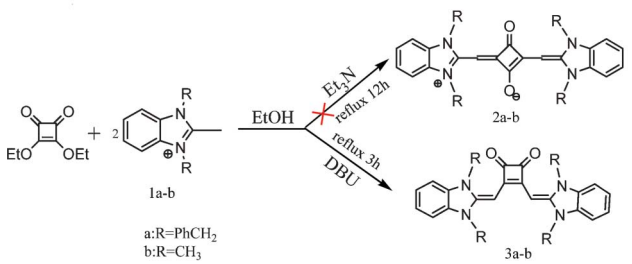

Scheme 1 The reaction of benzimidazole salt with 3,4-diethyl squarate.

benzimidazole salt **1a** with 3,4-diethyl squarate in the presence of a frequently-used base (triethylamine (Et_3N)) in EtOH (Scheme 1), however, no products formed after heating under reflux for 12 h, and **1a** did not react at all. Therefore, a fairly strong base was then used to catalyze the reaction. As a result, the reaction mixture turned from yellow to deep red instantly when diazabicycloundecene (DBU) was added and after a 3 h reflux a dull-red product was isolated with a 68% yield and crystallized by the slow evaporation method. To our surprise, the X-ray diffraction analysis of the product showed that the red product was 1,2-SQ **3a** (Fig. 1) instead of 1,3-SQ **2a**. Also, **3a** was characterized by various spectroscopic and analytical techniques: ^{1}H and ^{13}C NMR spectroscopy, FT-IR and elemental analysis.

The results show that we should draw to the thought that the basicity of the base has a large effect towards the products; this prompted us to use a stronger base to verify this inference. Sodium ethoxide (EtONa), as a common organic base, was used to catalyze the condensation reaction between **1a** and **1b** and 3,4-diethyl squarate. As expected, red deposits formed immediately as long as EtONa had been added and after a 3 h reflux the reactions were completed to produce **3a** and **3b** in 89% and 86% yields, respectively. Moreover, in these reactions, 1,3-SQs (**2a** and **2b**) were not observed. However, when squaric acid was reacted with **1a** and **1b** in EtOH solvent, no red product 1,2-SQs formed after heating under reflux for 3 h (Scheme 2). The weaker base pyridine was also used to catalyze the condensation reactions between **1a** and **1b** and 3,4-diethyl squarate; the mixture was always beige, and no red deposit formed in these reactions after heating under reflux

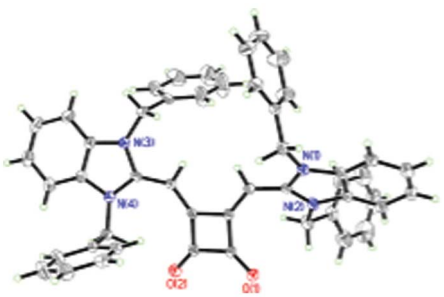

Fig. 1 The ORTEP diagram of **3a**.

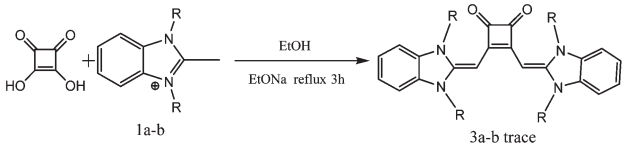

Scheme 2 The reaction between benzimidazole salt and squaric acid catalyzed byEtONa.

Table 1 The reaction of the benzimidazole salts (**1a** and **1b**) and 3,4-diethyl squarate catalyzed by various bases

	R	Base	Time (h)	Product	Yield (%)
1	$PhCH_2$	pyridine	12	**3a**	0
2	CH_3	pyridine	12	**3b**	0
3	$PhCH_2$	Et_3N	12	**3a**	0
4	CH_3	Et_3N	12	**3b**	0
5	$PhCH_2$	DBU	3	**3a**	68
6	CH_3	DBU	3	**3b**	61
7	$PhCH_2$	EtONa	3	**3a**	89
8	CH_3	EtONa	3	**3b**	86

for 12 h. No 1,2- or 1,3-SQs formed, which is similar to the reaction using Et_3N as the base (Table 1).

Based on the results above, we wanted to determine whether an inorganic base can be used to catalyze these reactions. The yields of the reactions utilizing various inorganic bases are presented in Table 2. The inorganic bases also can catalyze these condensation reactions and the basicity of the base worked in the same way as the organic bases: only trace amounts of **3a** and **3b** were observed (inspected by TLC cromatography) when weak inorganic bases ($NaHCO_3$, $KHCO_3$, Na_2CO_3 and K_2CO_3) were used after refluxing for 12 h. However, with 250 mol% strong base Cs_2CO_3, NaOH or KOH, the yields of **3a** and **3b** were dramatically improved towards to 76% and 73%, 81% and 75%, and 85% and 80%, respectively.

The absorption spectra of **3a** and **3b** in selected solvents are presented in Fig. 2A and 3A (also see the ESI†). The spectra

Table 2 The reaction of the benzimidazole salts (**1a** and **1b**) and 3,4-diethyl squarate catalyzed by various inorganic bases

	R	Base	Time (h)	Product	Yield (%)
1	$PhCH_2$	$NaHCO_3$	12	**3a**	trace
2	CH_3	$NaHCO_3$	12	**3b**	trace
3	$PhCH_2$	$KHCO_3$	12	**3a**	trace
4	CH_3	$KHCO_3$	12	**3b**	trace
5	$PhCH_2$	Na_2CO_3	12	**3a**	trace
6	CH_3	Na_2CO_3	12	**3b**	trace
7	$PhCH_2$	K_2CO_3	12	**3a**	trace
8	CH_3	K_2CO_3	12	**3b**	trace
9	$PhCH_2$	Cs_2CO_3	3	**3a**	76
10	CH_3	Cs_2CO_3	3	**3b**	73
11	$PhCH_2$	NaOH	3	**3a**	81
12	CH_3	NaOH	3	**3b**	75
13	$PhCH_2$	KOH	3	**3a**	85
14	CH_3	KOH	3	**3b**	80

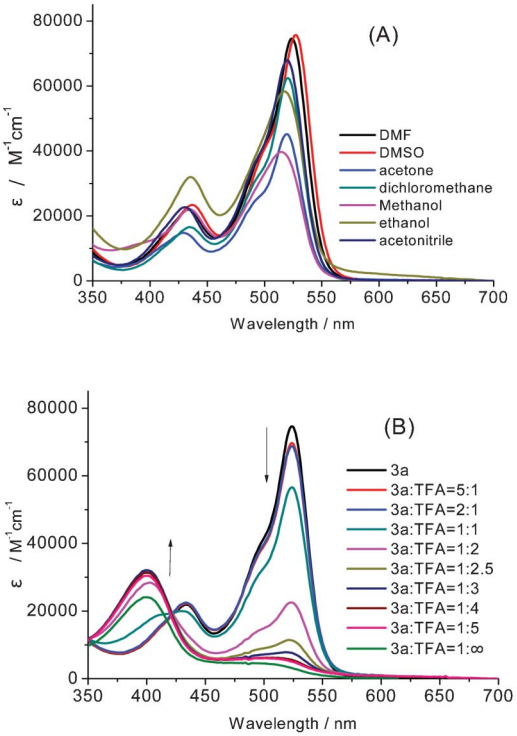

Fig. 2 The absorption spectra of the 1,2-SQ **3a** in various solvents (A). The absorption spectra change of **3a** in acetone upon the addition of different ratios of trifluoroacetic acid (TFA) (B).

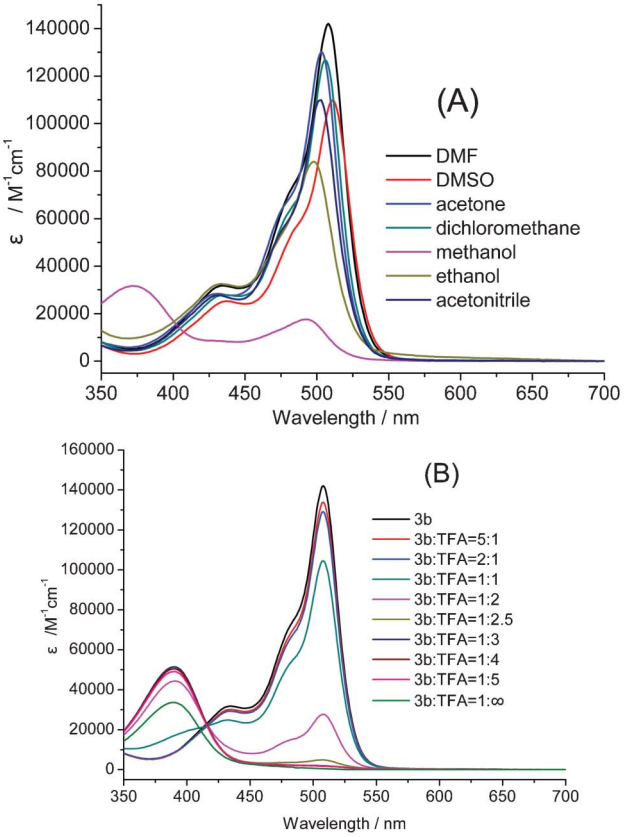

Fig. 3 The absorption spectra of the 1,2-SQ **3b** in various solvents (A). The absorption spectra change of **3a** in acetone upon the addition of different ratios of trifluoroacetic acid (TFA) (B).

indicate a solvent-dependent change in the absorption maxima and intensity of **3a**. The absorption maximum changes considerably in methanol compared with other solvents. The absorption coefficient of **3a** in dichloromethane is larger than in any other solvent. Similar results were also observed for **3b**. In Fig. 2B, the absorption peak at 524 nm decreases and that at 399 nm increases gradually as the concentration of TFA increases, which implies a strong pH dependence of the visible absorption spectra of **3a**. **3a** was also investigated by time-dependent density functional theory (TDDFT) calculations. Fig. S5, ESI† shows the calculated ground state structures and molecular orbitals of **3a**. From the TDDFT calculations, the long-wavelength absorption (524 nm) is mainly generated by the HOMO → LUMO transition. The short-wavelength absorption (433 nm) corresponds to the promotion of an electron from the HOMO-2 to the LUMO-1 (see Fig. S5, ESI†).

To examine the different reaction activities of various bases and their effect on the regioselectivity of this reaction, DFT calculations were performed to explore the detailed reaction mechanism (Scheme S3, ESI†).[17] In the first step of this reaction, **1b** reacted with different bases (EtONa, DBU, Et_3N and pyridine) to produce PRa complexes. Fig. 4A shows the energy profile for this deprotonation step. The H1 atom is attacked by the base (EtONa, DBU, Et_3N or pyridine) to produce an INa (INa1, INa2, INa3, or INa4) complex. All of these complexes have lower energies than the reactants (Fig. 2A). Because of the strong electron-donating ability of the lone pairs of electrons of the bases, the H1 atom is then transferred from **1b** to the base to afford 1a-base (INb) intermediates *via* transition states (TSa) (Fig. 4A). Also, Fig. 4A shows that TSa1 has a lower energy (−18.69 kcal mol^{-1}) than the reactants. However, the energy barriers of TSa2, TSa3 and TSa4 are 7.42, 14.84 and 16.37 kcal mol^{-1}, respectively, which are higher than those of the reactants. Subsequently, the products, PRa1, PRa2, PRa3 and PRa4 are formed from the INb complexes. Fig. 4A reveals that PRa1 and PRa2 are more stable than the reactants by 30.68 and 0.44 kcal mol^{-1}, respectively. However, the energies of PRa3 and Pra4 are 14.10 and 23.47 kcal mol^{-1} higher than those of the corresponding reactants. Because of the low energy barriers and exothermic characteristics, the reactions catalyzed by EtONa and DBU proceed easily. For Et_3N and pyridine, however, both reactions are strongly endothermic with relatively high energy barriers, and therefore it is understandable that these two reactions do not proceed readily. In addition, EtONa has the highest activity out of all of the bases used. These conclusions are consistent with the experimental results mentioned above where the reaction catalyzed by EtONa gives a high yield of 1,2-SQ (89%).

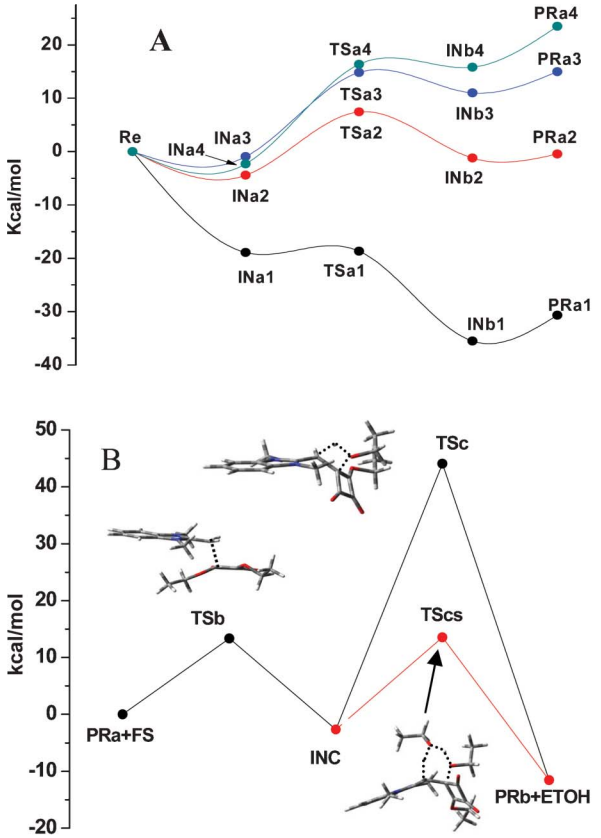

Fig. 4 The energy profiles for (A) the deprotonation of the benzimidazole salt by a base, and (B) the formation of PRb.

After deprotonation, the benzimidazole methylene (PRa) was formed (Scheme S1, ESI† and Fig. 4A). Because of the nucleophilicity of PRa, it is able to undergo a 1,4-conjugated attack at the squarate (FS) double bond (Fig. 4B). The step involves a transition state (TSb) that has a low active barrier (13.3 kcal mol^{-1}). An intermediate (INc) is then formed with an energy 2.31 kcal mol^{-1} above that of the reactants. The next step is a 1,5-proton shift between the methylene of PRa and the enolate (see Fig. 4B and Fig. S6 in the ESI†). Finally, the thermally-catalyzed elimination of ethanol gives exclusively PRb. In fact, this step (TSc) has a very high energy barrier (44.01 kcal mol^{-1}). This barrier is too large to enable the reaction to be conducted experimentally at an ambient temperature, so heating is required. Because the energy barriers involve proton transfer, we considered whether EtOH played an important role in this process. When EtOH was introduced as the proton transfer catalyst to assist in forming TScs (six-member ring transition state), the energy barrier was reduced considerably to 16.21 kcal mol^{-1} (Fig. 4B). This experiment also indicates that the yield and reaction rate would be increased considerably in ethanol compared with that in DMF catalyzed by DBU (Scheme 3).

Because of its nucleophilicity, PRa can continue to attack the C1 and C2 atoms of PRb through two reaction pathways: **I-A** and **I-B** (see Scheme S1, ESI†). In reaction pathway **I-A**, the C3

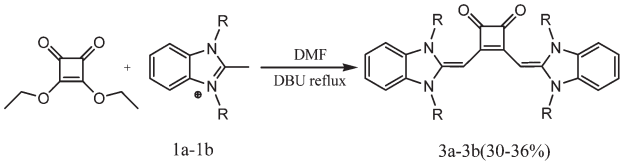

Scheme 3 The reaction of the benzimidazole salts (**1a** and **1b**) and 3,4-diethyl squarate catalyzed by DBU in dry DMF.

atom of PRa attacks the C1 atom of PRb to produce an intermediate INd. This process involves the transition state TSd with an energy barrier of 16.3 kcal mol^{-1} (Fig. 5 and Fig. S8, ESI†). After INd, the transition state TSe with an energy 37.58 kcal mol^{-1} above that of the reactants forms (Fig. S8, ESI†). TSe involves a proton transfer (H8) between the O9 and C7 atoms, and leads to products **3b** and EtOH. When EtOH is introduced as a cocatalyst, the energy barrier (TSes) decreases to 18.49 kcal mol^{-1}.

As displayed in Fig. 6 and Fig. S9 ESI,† in reaction pathway **I-B**, the C3 atom of PRa attacks the *para*-C2 atom of PRb to produce an intermediate INe *via* the transition state TSf with an energy barrier of 16.12 kcal mol^{-1}. After INe, a transition state TSg involving proton transfer (H8) from PRa to PRb with an energy barrier of 45.12 kcal mol^{-1} occurs. When EtOH is introduced as a proton transfer catalyst to assist this step, the energy barrier was reduced to 17.32 kcal mol^{-1}. In the next step, an OH group on the C2 atom transfers to the C1 atom. This process proceeds *via* the transition state TSh, which is 36.1 kcal mol^{-1} higher in energy than the reactants. After TSh, INg is formed with an energy of 3.07 kcal mol^{-1} above that of

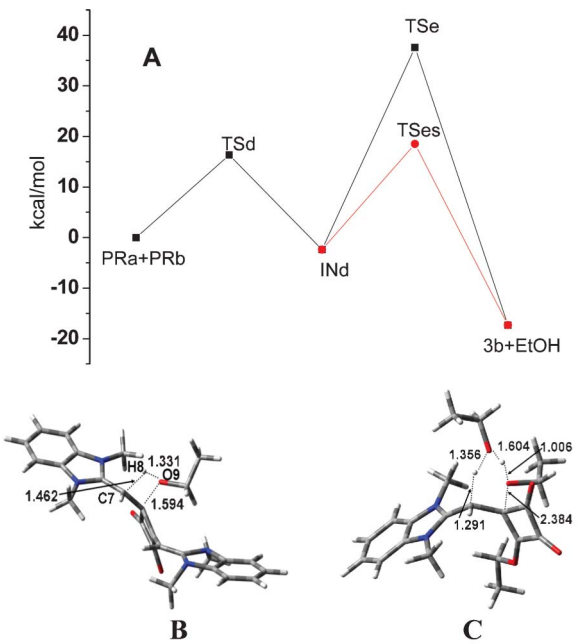

Fig. 5 The energy profiles for the formaction of **3b** (pathway: **I-A**) and the structures of the transition states (B: TSe, C: TSes).

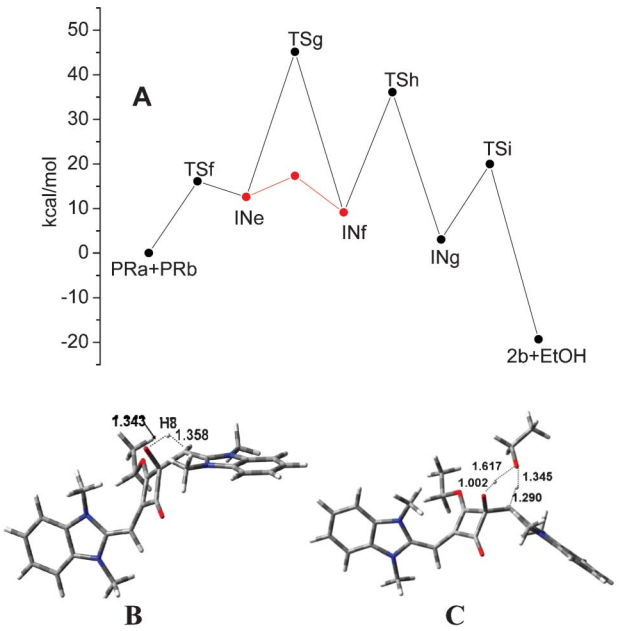

Fig. 6 The energy profiles for the formaction of **2b** (pathways: **I-B**) and the structures of transition states (B: TSg; C: TSgs).

the reactants. The last step for this pathway is a proton transfer from the OH group on C1 to the O atom of the ethyoxyl. This process results in the product **2b** *via* transition state TSi. The computed activation barrier for TSi is 19.97 kcal mol^{-1}. From the analyses above, it can be concluded that pathway **I-A** is the favorable reaction route, because its highest activation barrier (17.58 kcal mol^{-1}) is lower than that of pathway **I-B** (36.1 kcal mol^{-1}). This explains well the high regioselectivity for 1,2-SQs (**3a** and **3b**) in our experiments.

Conclusions

In summary, a method to prepare 1,2-benzimidazole squaraines in high yields *via* a one step reaction is developed. The yield of 1,2-benzimidazole squaraines is up to 89%. The total reaction mechanism is explored by DFT calculations. By combining the experimental and computational findings, we proposed a chemical regulation method to change the regioselectivity of the product. Our experimental and theoretical studies agree well with each other, paving a practical way to synthesize 1,2-squaraines in high yields. The syntheses of other 1,2-SQ complexes will be reported in the future.

Experimental section

Calculation details

The geometrical optimization, including transition-structure searches, was carried out with the standard 6-311G(d,p) basis set by using the three-parameter hybrid functional developed by Becke in the formulation implemented in the Gaussian 09 program[17] (B3LYP), which is slightly different from the original proposed by Becke.[18] The transition states are ascertained by vibrational analysis with only one imaginary frequency mode. In the case of TS, the vibration associated with the imaginary frequency was checked to correspond with a movement in the direction of the reaction coordinate.[19] The values of the relative energies, ΔE, have been calculated on the basis of the total energies of the stationary points. The solvent effects have been considered using a relatively simple self-consistent reaction field (SCRF) method, based on the polarizable continuum model (PCM).[20] The solvent used in this calculation is ethanol.

General remarks

All starting chemicals and solvents were purchased from commercial suppliers and used as received unless explicitly stated. Absorption spectrometry was performed using a Gold S54T spectrophotometer of Lengguang Company. Melting points were determined in open capillaries. ^{1}H NMR and ^{13}C NMR spectra were measured on a Bruker AVANCE 400 spectrometer in DMSO-d6 using TMS as an internal standard. The crystals for X-ray diffraction analysis were grown in dichloromethane by adding *n*-hexane to slowly diffuse. The X-ray diffraction experiment was carried out using a Bruker SMART APEX-II Single-crystal diffractometer.

The synthesis of 2-methyl benzoimidazole (a)

Phenylene diamine (0.3 mol, 32.4 g) and acetic acid (1 mol, 60 ml) were refluxed for 2 h. Ice and KOH were added to pH = 8–10 and a light violet solid filtered out. Then active carbon was used and recrystallized from water to giving 2-methyl benzoimidazol (**a**) as light yellow needle crystals (30 g, yield 77%), m.p 176–178 °C.[21]

The synthesis of 1,3-dibenzyl-2-methyl-benzimidazolium chloride (1a)

To a solution of 2-methylbenzimidazole (1 g, 7.57 mmol) in DMF (20 ml) benzyl chloride (2.66 ml, 22.7 mmol), potassium carbonate (1.25 g, 9.08 mmol) and a catalytic amount of tetra-*n*-butylammonium bromide was added. The mixture was stirred at room temperature for 24 h. The solution was filtered and the solvent was removed under reduced pressure. The residue was recrystallized from ethanol to afford 1,3-dibenzyl-2-methyl-benzimidazolium chloride (**1a**) as colorless amorphous crystals (0.8 g, yield 27%), m.p 312–314 °C;[22] ^{1}H NMR (400 MHz, DMSO-d6 δ): 7.92 (d, J = 1.67 Hz, 2H), 7.57 (d, J = 0.76 Hz, 2H), 5.81 (s, 4H), 7.36 (s, 10H) 2.99 (s, 3H); ^{13}C NMR (400 MHz, DMSO-d6 δ): 152.9 (1C), 134.6 (2C), 131.5 (2C) 129.4 (4C) 128.8 (4C), 127.49 (2C), 126.8 (2C), 113.8 (2C), 48.8 (2C), 11.5(1C).

The synthesis of 1,2,3-trimethyl benzimidazolium iodide (1b)

In a 250 ml round bottomed flask, Na (0.04 mol 0.9 g) was dissolved in 16 ml ethanol. After this 2-methyl benzimidazole (0.04 mol 5.2 g), 100 ml benzene and MeI (0.12 mol 7.5 ml) were added successively, and the mixture was refluxed for 18 h. The mixture was then allowed to cool to room temperature and the solvent was removed under reduced pressure. The crude product was purified by recrystallization from 95% ethanol to

afford 1,2,3-trimethyl benzimidazolium iodide (**1b**) as colorless needle crystals (9.2 g, yield 80%), m.p 258–259 °C;[23] ^{1}H NMR (400 MHz, DMSO-d6 δ): 7.97 (dd, J = 5.97, 2.93 Hz, 2H), 7.62 (dd, J = 6.01, 2.83 Hz, 2H), 3.99 (d, J = 14.04 Hz, 6H), 2.85 (s, 3H); ^{13}C NMR (400 MHz, DMSO-d6 δ): 152.7 (1C), 131.8 (2C), 126.2 (2C), 113.1(2C), 32.2 (2C), 11.1(1C).

A general procedure for the synthesis of 1,2-squaraines

All of the experiments described above were performed according to the following general procedure. A mixture of 2 mmol of squaric acid in 30 ml anhydrous ethanol was refluxed at 100 °C for 3 h under a nitrogen atmosphere. Then, the solvent was removed under reduced pressure and an other 30 ml steamed anhydrous ethanol was added. The mixture was refluxed for 30 min and the solvent was removed again. This was repeated for at least three times in order to get diethyl squarate generated completely. Base (10 mmol organic base: EtONa, DBU, Et_3N or pyridine; 5 mmol inorganic base: $NaHCO_3$, $KHCO_3$, Na_2CO_3, K_2CO_3, Cs_2CO_3, NaOH or KOH), 4 mmol of the benzimidazole salt and 15 ml anhydrous ethanol were added, and the mixture was refluxed for 3 h, and then allowed to cool to room temperature. The crude reaction mixture is inspected by TLC chromatography. The products were determined by comparison with the analytical samples of the various squaraines obtained by the procedures described in detail in the following paragraph.

The synthesis of 3,4-bis((1,3-dibenzyl-1*H*-benzo[d]imidazol-2(3H)-ylidene)methyl) cyclobut-3-ene-1,2-dione (3a)

A mixture of squaric acid (2 mmol, 228 mg) in 30 ml anhydrous ethanol was refluxed at 100 °C for 3 h under a nitrogen atmosphere. Then, the solvent was removed under reduced pressure and an other 30 ml steamed anhydrous ethanol was added. The mixture was refluxed for 30 min and the solvent was removed again. This was repeated for at least three times in order to make as much diethyl squarate as possible. In the meantime Na (230 mg, 10 mmol) was dissolved in 10 ml anhydrous ethanol, and the solution of sodium ethoxide **1a** (4 mmol, 1.39 g), and 15 ml anhydrous ethanol was added. The mixture turned to deep red at once and then was refluxed for 3 h. the solvent was removed under reduced pressure and 15 ml isopropanol was added to separate the garnet solid out. The solution was filtered and the residue was washed by isopropanol, ether and petroleum ether alternately to give **3a** as a garnet solid (1.25 g, yield 89%). M.p 217–218 °C; ^{1}H NMR (400 MHz, DMSO-d6 δ): 7.35 (dd, J = 4.88, 2.57 Hz, 4H), 7.17 (t, J = 6.53 Hz, 12H), 7.11–7.07 (m, 4H), 7.01 (d, J = 6.91 Hz, 8H), 5.42 (s, 8H), 4.70 (s, 2H); ^{13}C NMR (400 MHz, DMSO-d6 δ): 189.4 (2C), 170.9 (2C), 151.1 (2C), 136.6 (4C), 133.3 (4C), 129.1 (8C), 128.0 (8C), 127.2 (4C), 123.3 (4C), 110.3 (4C), 65.9 (2C), 47.8 (4C); anal. Calcd for **3a**: C, 81.95; H, 5.41; N, 7.96. Found: C, 81.73; H, 5.87; N, 7.67.

The synthesis of 3,4-bis((1,3-dimethyl-1*H*-benzo[d]imidazol-2(3H)-ylidene)methyl) cyclobut-3-ene-1,2-dione (3b)

A mixture of squaric acid (2 mmol, 228 mg) in anhydrous ethanol was reacted in the same way as the steps described above. In the meantime Na (230 mg, 10 mmol) was dissolved in 10 ml anhydrous ethanol. A solution of sodium ethoxide, **1b** (4mmol, 1.15 g) and 15 ml anhydrous ethanol was added, and the mixture turned from yellow to blood red immediately. The mixture was refluxed for 3 h and then allowed to cool to room temperature. The solution was filtered and the residue was washed by ethanol, ether and petroleum ether in turn to give a pure bright red solid product **3b** (684 mg, yield 86%). M.p. > 300 °C; ^{1}H NMR (400 MHz, DMSO-d6 δ): 7.39–7.34 (m, 4H), 7.22–7.18 (m, 4H),4.75–4.72 (m, 2H), 3.67 (s, 12H); anal. Calcd for **3b**: C, 72.36; H, 5.53; N, 14.07. Found: C, 72.25; H, 5.64; N, 14.03.

Acknowledgements

The support of the National Natural Science Foundation of China (10947171 and 21103082) is gratefully acknowledged.

Notes and references

1 (*a*) J. D. Park, S. Cohen and J. R. Lacher, *J. Am. Chem. Soc.*, 1962, **84**, 2919–2922; (*b*) J. J. McEwen and K. Wallace, *Chem. Commun.*, 2009, 6339–6351.

2 (*a*) F. Silvestri, M. D. Irwin, L. Beverina, A. Facchetti, G. A. Pagani and T. J. Marks, *J. Am. Chem. Soc.*, 2008, **130**, 17640–17641; (*b*) G. D. Wei, R. R. Lunt, K. Sun, S. Y. Wang, M. E. Thompson and S. R. Forrest, *Nano Lett.*, 2010, **10**, 3555–3559; (*c*) U. Mayerhöfer and F. Wüthner, *Chem. Sci.*, 2012, **3**, 1215–1220.

3 (*a*) A. Ajayaghosh, P. Chithra and R. Varghese, *Angew. Chem., Int. Ed.*, 2007, **46**, 230–233; (*b*) U. Mayerhöfer and F. Wüthner, *Angew. Chem., Int. Ed.*, 2012, **51**, 5615–5619; (*c*) S. Sreejith, P. Carol, P. Chithra and A. Ajayaghosh, *J. Mater. Chem.*, 2008, **18**, 264–274.

4 (*a*) X. Zhang, J. Jie, W. Zhang, C. Zhang, L. Luo, Z. He, X. Zhang, W. Zhang, C. Lee and S. Lee, *Adv. Mater.*, 2008, **20**, 2427–2432; (*b*) K. Y. Law, *Chem. Rev.*, 1993, **93**, 449–486; (*c*) H. Choi, J.-J. Kim, K. Song, J. Ko, M. K. Nazeeruddin and M. Grätzel, *J. Mater. Chem.*, 2010, **20**, 3280–3286.

5 (*a*) A. Dualeh, J. H. Delcamp, M. K. Nazeeruddin and M. Grätzel, *Appl. Phys. Lett.*, 2012, **100**, 173512; (*b*) M. Emmelius, G. Pawlowski and H. Vollmann, *Angew. Chem., Int. Ed. Engl.*, 1989, **28**, 1445–1471; (*c*) R. Petermann, M. Tian, S. Tatsuura and M. Furuki, *Dyes Pigm.*, 2003, **57**, 43–54.

6 E. C. P. Smits, S. Setayesh, T. D. Anthopoulos, M. Buechel, W. Nijssen, R. Coehoorn, P. W. M. Blom, B. de Boer and D. M. de Leeuw, *Adv. Mater.*, 2007, **19**, 734–738.

7 (*a*) A. Piechowski, G. Bird, D. Morel and E. Stogryn, *J. Phys. Chem.*, 1984, **88**, 934–950; (*b*) K. Liang, K.-Y. Law and D. G. Whitten, *J. Phys. Chem.*, 1995, **99**, 16704–16708; (*c*) J.-H. Yum, P. Walter, S. Huber, D. Rentsch, T. Geiger, F. Nuesch, F. D. Angelis, M. Grätzel and M. K. Nazeeruddin, *J. Am. Chem. Soc.*, 2007, **129**, 10320–10321; (*d*) Y. Shi, R. B. M. Hill, J.-H. Yum, A. Dualeh, S. Barlow, M. Grätzel, S. R. Marder and M. K. Nazeeruddin, *Angew. Chem., Int. Ed.*, 2011, **50**, 6619–6621; (*e*) U. Mayerhöfer, K. Deing, K. Gruβ, H. Braunschweig, K. Meerholz and F. Wüthner, *Angew. Chem., Int. Ed.*, 2009, **48**, 8776–8779; (*f*) G. Wei, X. Xiao, S. Wang, J. D. Zimmerman, K. Sun, V. V. Diev, M.

E. Thompson and S. R. Forrest, *Nano Lett.*, 2011, **11**, 4261–4264; (*g*) X. Xiao, G. Wei, S. Wang, J. D. Zimmerman, C. K. Renshaw, M. E. Thompson and S. R. Forrest, *Adv. Mater.*, 2012, **24**, 1956–1960.

8 (*a*) E. Arunkumar, C. C. Forbes, B. C. Noll and B. D. Smith, *J. Am. Chem. Soc.*, 2005, **127**, 3288–3289; (*b*) U. Mayerhöfer, B. Fimmel and F. Wüthner, *Angew. Chem., Int. Ed.*, 2012, **51**, 164–167; (*c*) J. M. Baumes, J. J. Gassensmith, J. Giblin, J.-J. Lee, A. G. White, W. J. Culligan, W. M. Leevy, M. Kuno and B. D. Smith, *Nat. Chem.*, 2010, **2**, 1025–1030.

9 (*a*) S. Cohen, J. R. Lacher and J. D. Park, *J. Am. Chem. Soc.*, 1959, **81**, 3480–3481; (*b*) J. D. Park, S. Cohen and J. R. Lacher, *J. Am. Chem. Soc.*, 1962, **84**, 2919–2922; (*c*) S. Cohen and S. G. Cohen, *J. Am. Chem. Soc.*, 1966, **88**, 1533–1536.

10 (*a*) M. B. Onaran, A. B. Comeau and C. T. Seto, *J. Org. Chem.*, 2005, **70**, 10792–10803; (*b*) Y. Xu, N. Yamamoto, D. I. Ruiz, D. S. Kubitz and K. D. Janda, *Bioorg. Med. Chem. Lett.*, 2005, **15**(19), 4304–4307; (*c*) A. Tevyashova, F. Sztaricskai, G. Batta, P. Herczegh and A. Jeney, *Bioorg. Med. Chem. Lett.*, 2004, **14**(18), 4783–4789; (*d*) J. R. Porter, S. C. Archibald, K. Childs, D. Critchley, J. C. Head, J. M. Linsley, T. A. Parton, M. K. Robinson, A. Shock, R. J. Taylor, G. J. Warrellow, R. P. Alexander and B. Langham, *Bioorg. Med. Chem. Lett.*, 2002, **12**(7), 1051–1054.

11 J. Xie, A. B. Comeau and C. T. Seto, *Org. Lett.*, 2004, **6**, 83–86.

12 (*a*) A. T. Blomquist and E. A. L. Lancette, *J. Am. Chem. Soc.*, 1961, **83**, 1387–1391; (*b*) S. Cohen and S. G. Cohen, *J. Am. Chem. Soc.*, 1966, **88**, 1533–1536.

13 (*a*) L. Beverina and P. Salice, *Eur. J. Org. Chem.*, 2010, 1207–1225; (*b*) U. Mayerhöfer, M. Gänger, M. Stolte, B. Fimmel and F. Wüthner, *Chem.–Eur. J.*, 2013, **19**, 218–232; (*c*) K-Y. Law and B. F. Court, *Can. J. Chem.*, 1986, **64**, 2267–2273; (*d*) A. Treibs and K. Jacob, *Justus Liebigs Ann. Chem.*, 1966, **699**, 153–167.

14 D. Yang, Z. Guan, L. Yang, Y. Huang, Q. Wei, Z. Lu and J. Yu, *Sol. Energy Mater. Sol. Cells*, 2012, **105**, 220–228.

15 R. R. Avirah, K. Jyothish, C. H. Suresh, E. Suresh and D. Ramaiah, *Chem. Commun.*, 2011, **47**, 12822–12824.

16 E. Ronchi, R. Ruffo, S. A. Rizzato Albinati, L. Beverina and G. A. Pagani, *Org. Lett.*, 2011, **13**, 3166–3169.

17 M. J. Frisch, G. W. Trucks, H. B. Schlegel, G. E. Scuseria, M. A. Robb, J. R. Cheeseman, G. Scalmani, V. Barone, B. Mennucci, G. A. Petersson, H. Nakatsuji, M. Caricato, X. Li, H. P. Hratchian, A. F. Izmaylov, J. Bloino, G. Zheng, J. L. Sonnenberg, M. Hada, M. Ehara, K. Toyota, R. Fukuda, J. Hasegawa, M. Ishida, T. Nakajima, Y. Honda, O. Kitao, H. Nakai, T. Vreven, J. A. Montgomery Jr, J. E. Peralta, F. Ogliaro, M. Bearpark, J. J. Heyd, E. Brothers, K. N. Kudin, V. N. Staroverov, T. Keith, R. Kobayashi, J. Normand, K. Raghavachari, A. Rendell, J. C. Burant, S. S. Iyengar, J. Tomasi, M. Cossi, N. Rega, J. M. Millam, M. Klene, J. E. Knox, J. B. Cross, V. Bakken, C. Adamo, J. Jaramillo, R. Gomperts, R. E. Stratmann, O. Yazyev, A. J. Austin, R. Cammi, C. Pomelli, J. W. Ochterski, R. L. Martin, K. Morokuma, V. G. Zakrzewski, G. A. Voth, P. Salvador, J. J. Dannenberg, S. Dapprich, A. D. Daniels, O. Farkas, J. B. Foresman, J. V. Ortiz, J. Cioslowski and D. J. Fox, *Gaussian 09*, Revision A02, Wallingford CT, 2009.

18 (*a*) A. D. Becke, *J. Chem. Phys.*, 1993, **98**, 5648; (*b*) C. Lee, W. Yang and R. Parr, *Phys. Rev. B*, 1988, **37**, 785.

19 J. W. Mciver, *Acc. Chem. Res.*, 1974, **7**, 72.

20 (*a*) M. Cossi, V. Barone and R. Cammi Tomasi, *Chem. Phys. Lett.*, 1996, **255**, 327; (*b*) M. T. Cances, V. Mennunci and J. Tomasi, *J. Chem. Phys.*, 1997, **107**, 3032; (*c*) V. Barone, M. Cossi and J. Tomasi, *J. Comput. Chem.*, 1998, **19**, 404.

21 K. F. Ansari and C. Lal, *Eur. J. Med. Chem.*, 2009, **44**, 4028–4033.

22 Z. Shi, J. L. Qiang and Z. Li, *Chin. Sci. Bull.*, 2001, **46**, 393–395.

23 N. A. Zakhavova, B. A. Poral-Koshlts and L. S. E-Fros, *Zhur Obshei Khim*, 1953, **23**, 1225–1230.